Wireless Personal Communications **10:** 33–52, 1998.

Performance of RS-Coded DS/CDMA Microcellular Systems with *M*-ary Orthogonal Signaling

A.C. IOSSIFIDES and F-N. PAVLIDOU
Aristotle University of Thessaloniki, School of Engineering, Dept. of Electrical and Computer Engineering, Telecommunications Division, P.O. Box 1641, 54 006 Thessaloniki, Greece

Abstract. This paper investigates the application of Reed-Solomon coding on DS/CDMA systems with M-ary orthogonal signaling for the reverse link of a microcellular environment. The performance of voice and data communications are analytically evaluated for a Rician or Rayleigh faded channel with lognormal shadowing and a two-slope path loss model. The effects of sectorization and antenna diversity are also considered. Numerical results, in terms of bit error probability and throughput, show that with proper selection of the coding rate and spreading, the proposed system presents enhanced performance with moderate complexity.

Keywords: DS/CDMA, RS coding, throughput, M-ary orthogonal signaling.

1. Introduction

Direct sequence code division multiple access (DS/CDMA) has already been established as a strong candidate for third-generation mobile and personal communication systems. Inherently offering soft capacity by smooth performance degradation with increasing load, microcellular DS/CDMA systems have proved capable servicing a large number of voice or data users when properly designed to incorporate power control, sectorization, and voice activity monitoring [1, 2]. Among various configurations studied during the last decade, DS/CDMA with M-ary orthogonal signaling was found to be a rather effective scheme for either indoor or outdoor mobile cellular and microcellular communications [3–11]. DS/CDMA with M-ary orthogonal signaling may be accomplished in several ways. The most frequently considered in the literature are: by mapping information symbols to random orthogonal complex spreading sequences with elements usually taken from the r th roots of unity [3–5]; by mapping the information symbols to Walsh/Hadamard (W/H) orthogonal functions which are spread by long spreading sequences [6–11]. Concatenated W/H and m sequences as spreading sequences have also been used [12].

Channel coding is strictly associated with signaling and it is much more effective, from the capacity or throughput perspective, for CDMA systems than for conventional systems [13]. As a drawback, added redundancy further increases the already spread bandwidth and thus, channel coding needs to be carefully designed to increase the total spectrum efficiency. The role of channel coding becomes more important when considering the reverse (from mobile to base station) link where coherent reception is out of the question. Recently, in [6–8], optimal convolutional codes were used for M-ary orthogonal DS/CDMA systems, while trellis-coded modulation over a biorthogonal set was proposed in [14].

RS codes have been considered very efficient when used in conjunction with M-ary orthogonal signaling in conventional (not CDMA) systems [15, 16]. They have also been found to be very effective for FH/SSMA systems, e.g. [17, 18]. This paper focuses on the application of RS coding on DS/CDMA systems with orthogonal signaling, a matter addressed for the first time in [11], extending the work presented there by including sectorization and throughput evaluation. Specifically, based on the second DS/CDMA M-ary orthogonal scheme aforementioned, the performance of either voice- or data-oriented systems is analyzed with powerful RS codes and simple bounded distance decoding for the noncoherent reverse link of a microcellular environment. The succeeding analysis and results show that RS coding in conjunction with M-ary orthogonal modulation is a very flexible and promising scheme for future wireless DS/CDMA systems.

Perfect slow power control is taken into account to overcome path loss and shadowing. The effect of short-term fast fading (considered as either Rayleigh or Rician) that may be frequency nonselective or selective, depending on the transmission bandwidth, is investigated. Shadowing is log-normally modeled and a two-slope path loss rule is incorporated. Diversity and sectorization are invoked to improve performance. Infinite interleaving is assumed.

In Section 2, the model of the system is described, including the transmitter, the different channel models, and the receiver. Performance analysis in terms of the bit error probability and throughput for voice- and data-oriented systems is presented in Section 3. Numerical and sample simulation results are given and analyzed in Section 4 and conclusions are given in Section 5.

2. System Model

The microcellular system under consideration consists of mobile users uniformly distributed in a hexagonal cellular structure. Each user communicates with the base station receiving the best signal and causes interference to all the other base stations. Two tiers of interfering cells are taken into account in the analysis (Figure 1a). Interference coming from farther users is negligible [2]. Voice users transmit with an information rate of 9.6 kb/s and allocate a bandwidth of about 1.23 MHz (similarly to [8, 11]). When data traffic is considered, coded information symbols form packets that are transmitted in a slotted manner to the base station. In this way, packets reach the base station almost simultaneously, but really asynchronously when viewed on a chip by chip basis because of different propagation delays. Synchronization among base stations is not considered and it is assumed that the total number of users in a slot duration remains constant. An information rate of 64 kb/s is considered with a total allocated bandwidth of about 8.2 MHz. Without any loss of generalization, a bandwidth expansion factor of 128 is considered for both cases.

In order to reduce multi-user interference and increase the maximum number of accommodated users per cell, sectorization can be taken into account. The antenna imperfections are modeled as in [2]; that is, if S is the number of sectors and υ is the overlap angle of the antennas, then the sectorization factor F_s may be defined as the ratio of total interference power in a sectorized and a nonsectorized system, that is

$$F_s = \frac{\text{sectorized-interference-power}}{\text{non-sectorized-interference-power}} = \left(\frac{1}{S} + \frac{2\upsilon}{360}\right) . \tag{1}$$

2.1. Transmitter

The transmitter of the proposed RS-coded DS/CDMA M-ary orthogonal configuration is very similar to that of [6–10], except for the encoding process where [11] was followed. b

source information bits of rate r_b are grouped and mapped to one of the $M = 2^b$ information symbols. The information symbols of rate $r_s = r_b / \log_2 M$ ks/s (ksymbols/s) enter a (n, k, t) RS encoder operating in $GF(M)$ with $n,\ k,\ t = \lfloor n - k \rfloor /2$ the block length, the number of information symbols each block contains, and the error correction capability of the code with bounded distance decoding, respectively. The output coded symbols of rate $r_{sc} = r_s / r_c$, where $r_c = k/n$, are interleaved and then mapped to one of the M Walsh-Hadamard orthogonal sequences which are further spread by an N length random sequence so that N/M is an integer. The transmitted signal by the k th user communicating with the q th base station may be expressed as

$$s_{q,k}(t) = Re\left\{u_m^{(q,k)}(t) \exp(j\omega_c t)\right\}, \tag{2}$$

where

$$u_m^{(q,k)}(t) = \sqrt{P_{q,k}} H_m^{(q,k)}\left(t - \tau_{q,k}\right) A^{(q,k)}\left(t - \tau_{q,k}\right) \exp\left(j\theta_{q,k}\right) \tag{3}$$

is the lowpass equivalent waveform with ω_c,$\tau_{q,k}$, and $\theta_{q,k}$ the carrier, access delay, and modulator phase, respectively, of the kth user in qth cell. $H_m^{(q,k)}(t)$ denotes the mth $(0 \leq m \leq M-1)$ transmitted Hadamard waveform of the kth user, given by

$$H_m^{(q,k)}(t) = \sum_{j=1}^{M} h_{m,j} P_{T_H}(t - jT_H) \tag{4}$$

with $h_{m,j}$ the jth element of the mth Hadamard sequence and $P_{T_H}(t)$ a rectangular pulse of unit amplitude and duration T_H. The spreading waveform $A^{(q,k)}(t)$ of the kth user consists of two quadrature components; that is, $A^{(q,k)}(t) = a_I^{(q,k)}(t) + a_Q^{(q,k)}(t) = \sum_{j=-\infty}^{\infty} a_{I,j}^{(q,k)} P_{T_c}(t - jT_c) + \sum_{j=-\infty}^{\infty} a_{Q,j}^{(q,k)} P_{T_c}(t - jT_c)$, where $a_{I,j}^{(q,k)}$ and $a_{Q,j}^{(q,k)}$ are the elements of the inphase and quadrature spreading sequences. $P_{T_c}(t)$ is the chip waveform, taken as a rectangular pulse of unit amplitude and duration T_c. The transmitted power, $P_{q,k}$, is properly adjusted by the slow power control procedure so that all intracell signals reach the base station with the same average power.

The total bandwidth expansion introduced by the modulator and the encoder is

$$\eta = \frac{W}{r_b} = \frac{N}{r_c \log_2 M}, \tag{5}$$

where W is the single-sided occupied spectrum. Assuming a constant bandwidth expansion factor of 128, several configurations may be derived by choosing a symbol set size M and then adjusting r_c and N so that N/M is an integer. Extended or shortened RS codes may arise in order to keep η constant. Some possible configurations for voice-oriented systems are given in Table 1. In order to keep the different configurations comparable for data-oriented packet transmission, a constant number of information bits per packet must be considered. In order to keep the number of code words transmitted per packet integer, a minimal difference of information bits per packet is allowed regarding different symbol sets. The number of bits L_b per packet, the number of symbols L_s per packet, the RS code, the resulting number of code words w per packet, and the spreading sequence length are given for various configurations in Table 2. The differences in number of bits per packet does not in any way change the validity of the comparative (between different configurations) results presented in Section 4.

Table 1. Some possible configurations for voice-oriented systems.

r_b(kb/s)	M	r_s(ks/s)	Code	r_{sc}(ks/s)	N
9.6	16	2.4	RS (16, 4, 6)	9.6	128
9.6	16	2.4	RS (16, 8, 4)	4.8	256
9.6	32	1.92	RS (30, 12, 9)	4.8	256
9.6	32	1.92	RS (30, 24, 3)	2.4	512
9.6	64	1.6	RS (63, 21, 21)	4.8	256
9.6	64	1.6	RS (63, 42, 10)	2.4	512

Table 2. Some possible configurations for data-oriented systems.

M	L_b	L_s	Code	w	N
16	256	64	RS (16, 4, 6)	16	128
16	256	64	RS (16, 8, 4)	8	256
32	240	48	RS (30, 12, 9)	4	256
32	240	48	RS (30, 24, 3)	2	512
64	252	42	RS (63, 21, 21)	2	256
64	252	42	RS (63, 42, 10)	1	512

2.2. Channel Model

2.2.1. *Multipath Fading*

The microcellular environment presents low RMS delay spread values in the order of 500 ns [19]. So, depending on the transmission bandwidth, the channel may be considered as either frequency selective for the wideband data-oriented system or frequency nonselective for the narrowband voice-oriented system. Additionally, when multipath fading arises, the delayed paths have usually less power than the first arriving path. Fading statistics, on the other hand, of the first arriving path may be Rician or Rayleigh, depending on the existence or not of an LOS component and may drop from one case to the other when the mobile moves around. Thus, both fading models are incorporated in the analysis as in [11, 12, 20]. In all cases, the channel is described by its complex equivalent impulse response, given by

$$h_{q,k}(t) = \sum_{l=1}^{L} \beta_{(q,k)l}\,\delta\left(t - t_{(q,k)l}\right) \exp\left(j\varphi_{(q,k)l}\right) \tag{6}$$

which is different for every mobile-base station link. $\beta_{(q,k)l}$ denotes the path amplitudes, $t_{(q,k)l}$ the path delays, and $\varphi_{(q,k)l}$ the path phases, modeled as uniform over $[0, 2\pi)$, of the lth path of the kth user's link with the qth base station. L denotes the number of resolvable paths.

Voice-Oriented Systems:
For voice-oriented systems, L equals one [8, 11]. The probability density function (pdf) of the path amplitude is

$$p_\beta(\beta) = 2\beta \exp(-R) \exp\left[-(R+1)\beta^2\right] I_0\left(2\beta\sqrt{R(R+1)}\right) \tag{7}$$

$$p_\beta(\beta) = 2\beta \exp\left(-\beta^2\right) \tag{8}$$

for Rice and Rayleigh fading, respectively, where R denotes the specular to diffuse component power ratio and $I_0(\cdot)$ is the modified Bessel function of the zeroth order. Note that both pdfs are normalized to have unit power, that is $E\left[\beta^2\right] = 1$. In this context, the power of the diffuse component (when Rice statistics are considered) equals $\frac{1}{R+1}$.

Data-Oriented Systems:
For data-oriented wideband systems, three paths are considered to exist as in [8, 11, 20] with the delayed paths being Rayleigh-distributed irrespective of the statistics of the first path which may be Rice or Rayleigh as in voice-oriented systems. The power of each delayed path is taken 6 dB less than the diffuse component of the first arriving path. Thus, for Rice fading, the power of the delayed paths equals $\frac{1}{4(R+1)}$, while for Rayleigh fading equals $\frac{1}{4}$.

2.2.2. *Shadowing and Path Loss*

The power of the received signal undergoes log-normal shadowing and path loss. Incorporating a two-slope path loss model which is the most probable to appear in microcellular environments, the received power at the reference base station ($q = 0$) from the kth user in qth cell is given by

$$P_{q,k}^{(0)} = P_{q,k} 10^{0.1\xi_{(q,k)0}} \frac{1}{r_{(q,k)0}^2 \left(1 + \frac{r_{(q,k)0}}{g}\right)^2}, \quad d > g \tag{9}$$

$$P_{q,k}^{(0)} = P_{q,k} 10^{0.1\xi_{(q,k)0}} \frac{1}{r_{(q,k)0}^2}, \quad d \leq g \tag{10}$$

where $\xi_{(q,k)0}$ is a Gaussian random variable with zero mean and standard deviation σ_G. $r_{(q,k)0}$ is the distance of the mobile to the reference base station and g is the breaking point distance of the path loss model. It is assumed that by proper positioning and height adjustment of the base stations' antennas, the breaking point distance equals the cell radius $\mathcal{R}$. Therefore, intracell-oriented signals reaching the reference base station undergo path loss given by (10), while out of cell-oriented signals undergo path loss given by (9). The slow power control procedure acts in order to overcome shadowing and path loss and is assumed to be perfect in that sense, while it does not change the short-term fading statistics. So, under the shadowing and path loss model described, the transmitted power of the kth user in qth cell is $P_{q,k} = 10^{-0.1\xi_{(q,k)q}} r_{(q,k)q}^2 P$, where P is the nominal power needed at the base station for effective demodulation.

2.3. RECEIVER

The signal received at the reference base station is the sum of all transmitting users from all the surrounding cells of the two tiers (18 interfering cells totally). When a single cell is considered, interference arises from in cell users only. In either case, the lowpass equivalent received signal is given by

$$r(t) = \sum_{q=0}^{18}\sum_{k=1}^{K_q}\sqrt{P\rho_{q,k}^{(0)}}\sum_{l=1}^{L}\beta_{(q,k)l}H_m^{(q,k)}\left(t-t_{(q,k)l}\right)A^{(q,k)}\left(t-t_{(q,k)l}\right)\exp\left(j\varphi_{(q,k)l}\right) + n(t) \quad (11)$$

where

$$\rho_{q,k}^{(0)} = 10^{0.1\left(\xi_{(q,k)0}-\xi_{(q,k)q}\right)}\frac{r_{(q,k)q}^2}{r_{(q,k)0}^2\left(1+r_{(q,k)0}/\mathcal{R}\right)^2}, \quad q\neq 0. \quad (12)$$

$\rho_{0,k}^{(0)} = 1$ for perfect power-controlled intracell users, while q takes only the zero value in (11) for single cell operations. $t_{(q,k)l}$ and $\varphi_{(q,k)l}$ are the delay and phase of the $(q,k)\,l$ signal incorporating both access plus channel delay and modulator plus channel phase. $n(t)$ is the complex white Gaussian noise process with two-sided spectral density $2N_0$.

The reduced desired signal power of the delayed multipaths in data systems, the use of a RAKE receiver based on noncoherent detection dubious and will not significantly improve (if at all) the performance. This is due to the noncoherent combining loss [8, 15]. Therefore, a single correlator receiver is used for both voice and data systems and dual antenna diversity is applied for performance enhancement [8]. The detector is identical to that given in [10] and consists of two branches (inphase and quadrature), each one with despreaders (for inphase and quadrature sequences) and a bank of envelope correlators matched to the M orthogonal Hadamard waveforms. Extending the results presented there, assuming that the delay of the reference user (user 0) of the reference cell is zero, and considering all the other delays relatively, the decision variable of the pth correlator when the mth waveform was transmitted is given by $D_p = \left|Z_p\right|^2$, where

$$\begin{aligned} Z_p &= Z_{p,I} + jZ_{p,Q} \\ &= \frac{1}{2\sqrt{T}}\int_0^T r(t)\,H_p^{(0,0)}(t)\,A^{(0,0)*}(t)\,dt \\ &= \sqrt{PT}\beta_{(0,0)1}\delta\left[H_m^{(0,0)}(t),H_p^{(0,0)}(t)\right]\exp\left(\varphi_{(0,0)1}\right) + I_{mu} + I_{in} + I_{out} + n' \end{aligned} \quad (13)$$

where $\delta\left[H_m^{(0,0)}(t),H_p^{(0,0)}(t)\right] = 0$ if $H_m^{(0,0)}(t)\neq H_p^{(0,0)}(t)$ and $\delta\left[H_m^{(0,0)}(t),H_p^{(0,0)}(t)\right] = 1$ if $H_m^{(0,0)}(t) = H_p^{(0,0)}(t)$. Additionally,

$$I_{mu} = \sqrt{\frac{P}{4T}}\sum_{l=2}^{L}\beta_{(0,0)l}\left[RH_{(0,0)}\left(t_{(0,0)l}\right)+\widehat{RH}_{(0,0)}\left(t_{(0,0)l}\right)\right]\exp\left(\varphi_{(0,0)l}\right) \quad (14)$$

$$I_{in} = \sqrt{\frac{P}{4T}}\sum_{k=1}^{K_0-1}\sum_{l=1}^{L}\beta_{(0,k)l}\left[RH_{(0,k)}\left(t_{(0,k)l}\right)\widehat{RH}_{(0,k)}\left(t_{(0,k)l}\right)\right]\exp\left(\varphi_{(0,k)l}\right) \quad (15)$$

$$I_{out} = \sqrt{\frac{P}{4T}}\sum_{q=1}^{18}\sum_{k=1}^{Kq}\sum_{l=1}^{L}\sqrt{\rho_{q,k}^{(0)}}\beta_{(q,k)l}\left[RH_{(q,k)}\left(t_{(q,k)l}\right)+\widehat{RH}_{(q,k)}\left(t_{(q,k)l}\right)\right] \cdot\exp\left(\varphi_{(q,k)l}\right) \quad (16)$$

are the multipath interference of the reference user's delayed paths, the multiple access interference of the reference cell, and the total intercell interference, respectively. Note that $L = 1$

and multipath interference does not exist for voice-oriented systems. K_q is the number of active users per cell. $RH_{(q,k)}(\cdot)$ and $\widehat{RH}_{(q,k)}(\cdot)$ are the partial continuous time cross-correlation functions between the pth orthogonal waveform/spreading sequence of the reference user and the νth orthogonal waveform/spreading sequence of the kth user at the qth cell, given by

$$RH_{(q,k)}(\tau) = \int_0^{\tau} H_{\nu-1}^{(q,k)}(t-\tau)\, A^{(q,k)}(t-\tau)\, H_p^{(0,0)}(t)\, A^{(0,0)*}(t)\, dt \tag{17}$$

$$\widehat{RH}_{(q,k)}(\tau) = \int_{\tau}^{T} H_{\nu}^{(q,k)}(t-\tau)\, A^{(q,k)}(t-\tau)\, H_p^{(0,0)}(t)\, A^{(0,0)*}(t)\, dt. \tag{18}$$

Finally, $n^{'} = n_I + jn_Q$, with n_I and n_Q zero mean Gaussian random variables with variance $N_0/2$.

The decision variables D_p $(0 \le p \le M-1)$ that come out of the correlators are mutually compared and the symbol corresponding to the maximum one is selected. After deinterleaving, the detected symbols form blocks of length corresponding to the RS code used and enter the decoder. Since no channel state information is preserved, bounded-distance decoding is performed.

3. Performance Analysis

Performance is predicted in terms of the bit error probability (BEP) for voice-oriented systems and in terms of throughput for data-oriented systems.

3.1. Bit Error Probability

Invoking the Gaussian approximation for the total interference and taking into account the analysis of [9] and [10] concerning the evaluation of the variance of the interference between the orthogonal waveforms, the variance of the interference terms is found to be

$$\sigma_{I_{mu}}^2 = \frac{PT}{3N} \sum_{l=2}^{L} E\left[\beta_{(0,0)l}^2\right] \tag{19}$$

$$\sigma_{I_{in}}^2 = \psi F_s \frac{PT}{3N} \sum_{k=1}^{K_0-1} \sum_{l=1}^{L} E\left[\beta_{(0,k)l}^2\right] \tag{20}$$

$$\sigma_{I_{out}}^2 = \psi F_s \frac{PT}{3N} \sum_{q=1}^{18} \sum_{k=1}^{K_q} \sum_{l=1}^{L} E\left[\rho_{q,k}^{(0)}\right] E\left[\beta_{(q,k)l}^2\right] \tag{21}$$

respectively, where $E[\cdot]$ denotes mean value and ψ is the voice activity factor. In the above equations, $L = 1$ for voice-oriented systems, while $\psi = 1$ for data-oriented systems. Additionally, $F_s = 1$ for nonsectorized systems. Assuming K users per cell, the total average signal to interference plus noise ratio was found to be

$$\gamma = \left[\frac{N_0}{E_b r_c \log_2 M} + \frac{1}{3N(R+1)} + F_s \frac{2(K-1)}{3N}\left(1 + \frac{1}{2(R+1)}\right) + F_s F_o \frac{2K}{3N}\left(1 + \frac{1}{2(R+1)}\right)\right]^{-1} \tag{22}$$

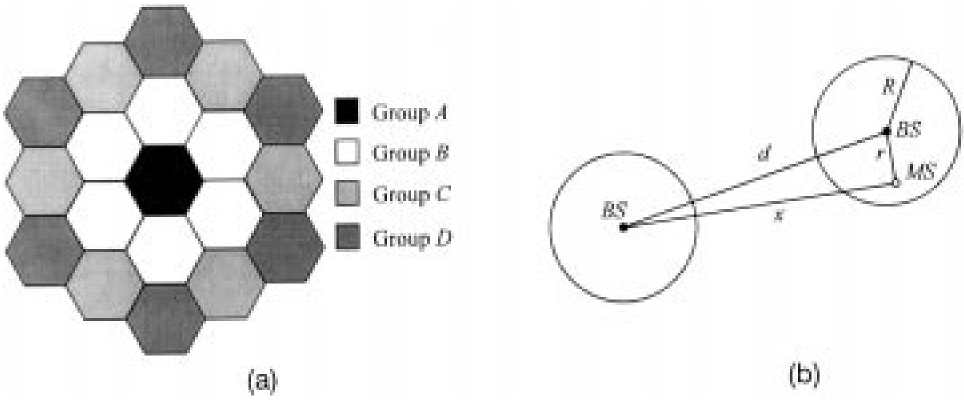

Figure 1. (a) Cellular structure under consideration with the four groups of interfering cells. (b) Geometry for intercell interference calculation.

for data-oriented systems and Rice fading ($R = 0$ for Rayleigh fading) and

$$\gamma = \left[\frac{N_0}{E_b r_c \log_2 M} + \psi F_s \frac{2(K-1)}{3N} + \psi F_s F_o \frac{2KF}{3N} \right]^{-1} \tag{23}$$

for voice-oriented systems either Rician or Rayleigh faded. In (22) and (23), F_o stands for the intercell interference factor ($F_o = 0$ for single cell systems), which consists of the sum of $E\left[\rho_{q,k}^{(0)}\right]$ of all interfering cells. To evaluate F_o, we use the geometry of Figure 1b. Assuming a uniform spatial traffic density in each cell and approximating hexagonal cells as circular ones with radius $\mathcal{R}$, the pdf of the distance $r \equiv r_{(q,k)q}$ of the kth user communicating with the qth base station is

$$p(r) = \begin{cases} 2r/\mathcal{R}, & r \le \mathcal{R} \\ 0, & otherwise \end{cases} \tag{24}$$

Referring to Figure 1b, we can write $x \equiv r_{(q,k)0} = \sqrt{d^2 + r^2 + 2dr\cos\phi}$ with ϕ uniform in $[0, 2\pi)$ and d the intercenter distance between cells. Therefore,

$$E\left[\rho_{q,k}^{(0)}\right] = \frac{1}{\pi \mathcal{R}^2} \int_0^{2\pi} \int_0^{\mathcal{R}} \frac{r^2}{x^2 (1 + x/\mathcal{R})^2} E\left[10^{0.1\left(\xi_{(q,k)0} - \xi_{(q,k)q}\right)}\right] r dr d\phi. \tag{25}$$

Since $\xi_{(q,k)0}$, $\xi_{(q,k)q}$ are independent, their difference has zero mean and variance $2\sigma_G^2$. Following the procedure of [1] with the constraint $\rho_{q,k}^{(0)} \le 1$ so that mobile users communicate with the base station receiving the highest power, results in

$$\begin{aligned} E\left[10^{0.1\left(\xi_{(q,k)0} - \xi_{(q,k)q}\right)}\right] &= \exp\left[(0.1\sigma_G \ln 10)^2\right] \\ &\cdot \left\{ 1 - Q\left[\frac{20 \log_{10} \frac{x(1+x/\mathcal{R})}{r}}{\sqrt{2\sigma_G^2}} - 0.1\sqrt{2\sigma_G^2} \ln 10 \right] \right\} \end{aligned} \tag{26}$$

Regarding their distance from the reference base station, the 18 interfering cells can be categorized into three groups (B, C, and D in Figure 1a) of six cells with intercenter distances $d = \sqrt{3}\mathcal{R}$, $3\mathcal{R}$, and $2\sqrt{3}\mathcal{R}$. Substituting for d in x and for x with respect to d, r, ϕ in (26) and then for (26) in (25), we can apply numerical integration with respect to r, ϕ to calculate $E\left[\rho_{q,k}^{(0)}\right]$. Summing over all the interfering cells gives F_0.

Given the average signal to noise plus interference ratio, the symbol error probability for K users per cell may be calculated by averaging the conditional symbol error probability with respect to the path amplitude. That is,

$$\begin{aligned} P_S(K) &= \int_0^\infty P_S(K/\beta)\, p_\beta(\beta)\, d\beta \\ &= \int_0^\infty \sum_{m=1}^{M-1} \binom{M-1}{m} \frac{(-1)^{m+1}}{m+1} \exp\left(-\frac{m\gamma}{m+1}\beta^2\right) p_\beta(\beta)\, d\beta \\ &= \sum_{m=1}^{M-1} \binom{M-1}{m} \frac{(-1)^{m+1}}{m+1+m\frac{\gamma}{R+1}} \exp\left[\frac{-Rm\gamma}{(R+1)(m+1)+m\gamma}\right] \end{aligned} \tag{27}$$

for Rice fading and

$$P_S(K) = \sum_{m=1}^{M-1} \binom{M-1}{m} \frac{(-1)^{m+1}}{m+1+m\gamma} \tag{28}$$

for Rayleigh fading. In this latter case, antenna diversity is also considered for performance improvement. When the simple and effective maximum output selection diversity of order D presented in [20] is used, the symbol error probability is given by

$$P_S(K) = \sum_{j=0}^{D} (-1)^j \binom{D}{j} \prod_{m=1}^{D(M-1)} \frac{m}{m+\frac{j}{1+\gamma}}. \tag{29}$$

Given the symbol error probabilities at the output of the detector and assuming perfect interleaving and fast fading, the postdecoding bit error probability is

$$P_{bc}(K) \simeq \frac{2^{\log_2 M-1}}{2^{\log_2 M}-1} \frac{1}{n} \sum_{i=t+1}^{n} i \binom{n}{k} P_S(K)^i \left[1-P_S(K)\right]^{n-i}. \tag{30}$$

3.2. THROUGHPUT

Assuming that the total number of users per cell is large enough to generate a Poisson-offered traffic, the probability $p_{tr}(k)$ of k simultaneous transmitted packets is

$$p_{tr}(k) = \frac{G^k}{k!} \exp(-G) \tag{31}$$

where G is the average offered traffic consisting of new generated plus retransmitted packets. Packets are retransmitted with exponential retransmission times until a positive acknowledgment of correct packet reception is received. Each packet is correctly received if all the code words it contains are successfully decoded. Therefore, the probability of packet success is given by

$$P_p(k) = \left[P_{CD}(k)\right]^w \tag{32}$$

where $P_{CD}(k)$ is the probability of correct code word decoding given by [15]

$$P_{CD}(k) = \sum_{i=0}^{t} \binom{n}{i} P_S(k)^i \left[1 - P_S(k)\right]^{n-i} . \tag{33}$$

When more than t errors are present in a code word, the decoder will either recognize the presence of an uncorrectable error pattern and thus acknowledgment will not be sent or incorrectly decode the packet, resulting in error. The probabilities of error detection P_{ED} and incorrect decoding P_{ICD} of a code word are given in the Appendix. P_{ICD} and the symbol error probability associated with it determine the postdecoding error probability for data-oriented systems. The throughput of the described system is defined as

$$S = \sum_{k=1}^{K_{\max}} k p_{tr}(k) P_p(k) \tag{34}$$

where $K_{\max} >> G$, theoretically infinite.

4. Results and Discussion

The use of RS codes in conjunction with M-ary orthogonal signaling for DS/CDMA systems gives, as described, the opportunity of constructing various schemes under a fixed bandwidth limitation and information rate. The main point of discussion is to find the optimum scheme by proper combination of M, r_c, and N that best suits the specific needs, in terms of performance and complexity, of the communication system under consideration. Extending the symbol set size M seems to result in a standard performance gain by allowing the use of lower rate codes or longer spreading sequences that reduce multi-user interference. This is true in high signal to noise plus interference ratios, but dubious in the low ones. On the other hand, the relationship of r_c and N for a fixed symbol set is very important and should be properly selected for a specific application.

In the results to be presented, the dB spread of the log-normal shadowing selected to be $\sigma_G = 8$ dB. Second order ($D = 2$) external diversity was at most used and $S = 3$ sectors were considered for sectorized configurations with an antenna overlap angle of $\upsilon = 20°$.

4.1. Voice-Oriented Systems

The above considerations are clearly illustrated in Figure 2 where a single-cell system is considered with Rayleigh fading and diversity for various system configurations at $E_b/N_0 =$ 20 dB. It should be noted that there is always a threshold with respect to the number of users, above which fixed M different configurations interchange their performance. This threshold is at about 150 users and 120 users for the $M = 32$ and $M = 64$ schemes, respectively. This means that for a relatively small number of users, stronger codes result in higher performance, while for a large number of simultaneous users greater spreading (greater N) is more important because of the reduction of the increased multi-user interference. Among all presented schemes, the $M = 64$ ones give the best performance results for voice communications. $K = 124$ and $K = 128$ users are accommodated with a BEP of 10^{-3} for the $RS(63, 21, 21)$ with $N = 256$ and the $RS(63, 42, 10)$ with $N = 512$ configurations, respectively. These two configurations referred to as **scheme 1** and **scheme 2**, respectively, will be considered next.

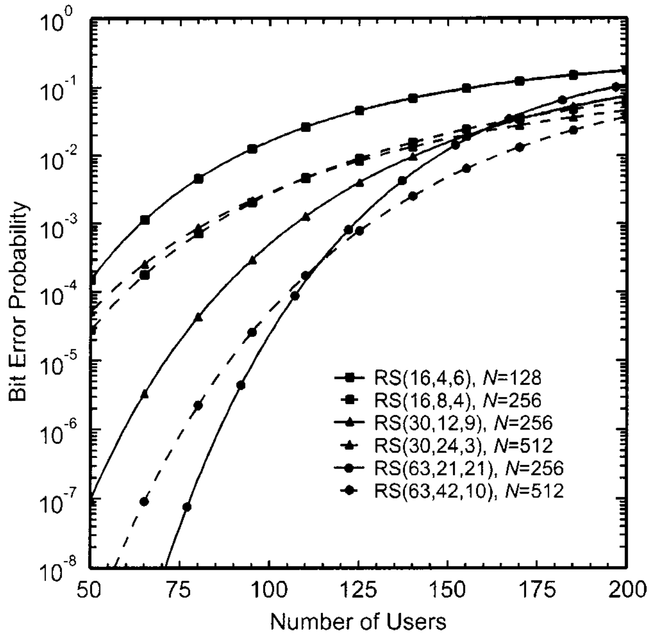

Figure 2. BEP of single-cell voice-oriented systems under Rayleigh fading for various RS coded schemes.

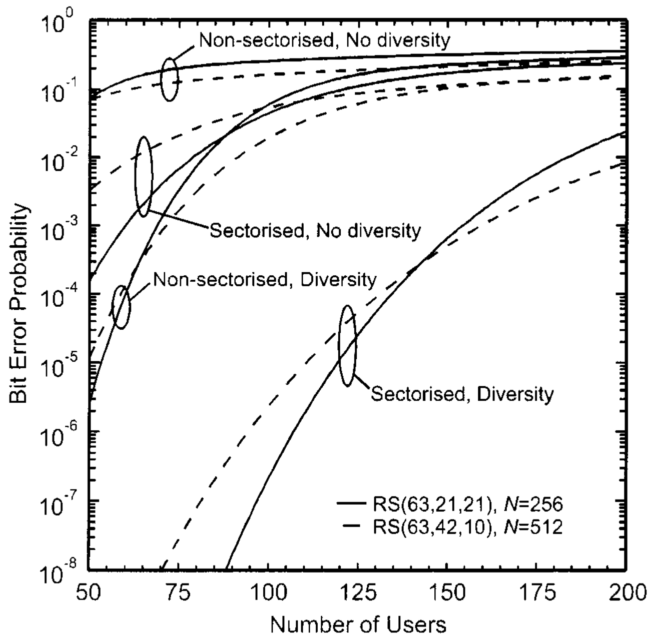

Figure 3. BEP of multicell voice-oriented systems under Rayleigh fading for the RS(63,21,21) and RS(63,42,10) schemes.

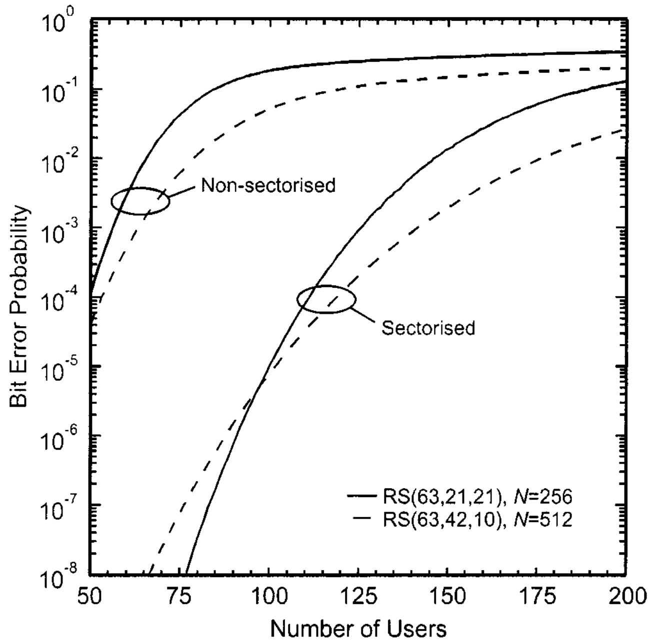

Figure 4. BEP of multicell voice-oriented systems under Rician fading for the RS(63,21,21) and RS(63,42,10) schemes.

Figure 3 presents the performance of the selected schemes under a Rayleigh fading environment in a multicell system incorporating either diversity, sectorization, or both at $E_b/N_0 =$ 20 dB. Systems with neither of them cannot service a significant number of users. 160 voice users can be accommodated with scheme 2 ($RS\,(63, 42, 10)$) which besides its higher capacity presents a smoother degradation in the region of BEP of interest. Two cases are of great interest in Figure 3. First, diversity and nonsectorized schemes outperform nondiversity and sectorized schemes in the region of interest. Thus, diversity is to be preferred over sectorization, which presents higher complexity and worse performance. Second, the $RS\,(63, 21, 21)$ scheme outperforms scheme 2 accommodating 20 users more (60 over 40) for sectorization and no diversity. This fact enhances the aforementioned considerations for careful selection of the proper scheme. Finally, comparison of Figures 2 and 3 shows that multicell systems present a 44% loss compared to single cell systems when diversity only is employed.

Figure 4 illustrates the performance of schemes 1 and 2 in Rician fading at $E_b/N_0 =$ 20 dB. Scheme 2 is clearly better at accommodating 63 and 142 users for nonsectorized and sectorized operations, respectively. In this context, sectorization gives a 125% performance gain over nonsectorized systems.

Figure 5 presents BEP results for scheme 2 under Rician or Rayleigh fading for various signal to noise ratios. With significant background noise, that is $E_b/N_0 = 10$ dB, 84 and 102 voice users can be accommodated under Rician fading with sectorization and Rayleigh fading with sectorization and diversity, respectively.

4.2. Data-Oriented Systems

Figure 6 presents comparative results of various configurations for a single cell Rician fading environment at $E_0/N_0 = 20$ dB. The $M = 64$ configurations present the highest throughput,

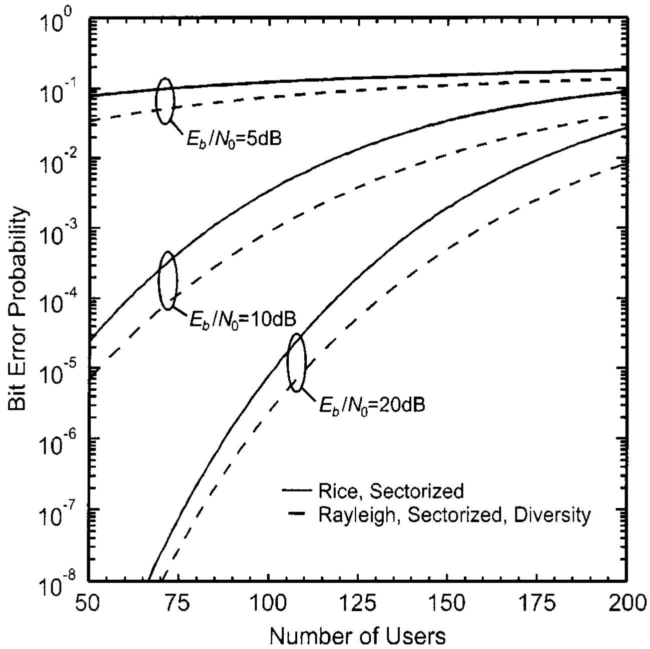

Figure 5. BEP of multicell voice-oriented systems for the RS(63,42,10) scheme and various signal to noise ratios.

attaining values 42.7 and 34.4 for schemes 2 and 1, respectively. Comparing Figures 6 and 7, it is shown that a 48% maximum throughput loss results for a multicell system in Rician fading. Sectorization enhances performance dramatically, resulting in 120 − −130% higher throughput values.

Figure 8 presents throughput results for schemes 1 and 2 over a Rayleigh fading microcellular environment at $E_b/N_0 = 20$ dB. Diversity proves better than sectorization again. It is worthy to note that for nondiversity systems (either sectorized or not) scheme 1, that is $RS(63, 21, 21)$, attains higher throughput values than the $RS(63, 42, 10)$ scheme. This is because when no diversity is used, higher signal to noise plus interference ratios are required for packet success and in higher signal to noise ratios the correcting capability of the code is more important than spreading. This relationship turns over when diversity is employed or when Rice fading occurs as shown in Figure 6. The maximum throughput values attained are 18.4 and 43.3 for Rayleigh fading with and without sectorization, respectively, for scheme 2. 22.3 and 52 are the corresponding values for Rician fading.

Figure 9 illustrates the effect of background noise at the throughput of scheme 2 for Rayleigh and Rician fading. At $E_b/N_0 = 10$ dB, the maximum throughput values attained are 30.2 and 35.5 for Rayleigh fading with sectorization and diversity and Rician fading with sectorization, respectively.

Figure 10 presents the probabilities of correct decoding, error detection, and incorrect decoding for the $RS(63, 42, 10)$ scheme under Rician and Rayleigh (without diversity) environments. For this coded scheme, the presented probabilities coincide with the corresponding packet probabilities. It is important to note that when the probability of correct decoding gets lower, error detection probability gets higher with almost an inverse rate. In both channel cases, however, the probability of incorrect decoding is almost stable at 10^{-9} for a large number of users. This means that the decoder almost always recognizes code-word errors

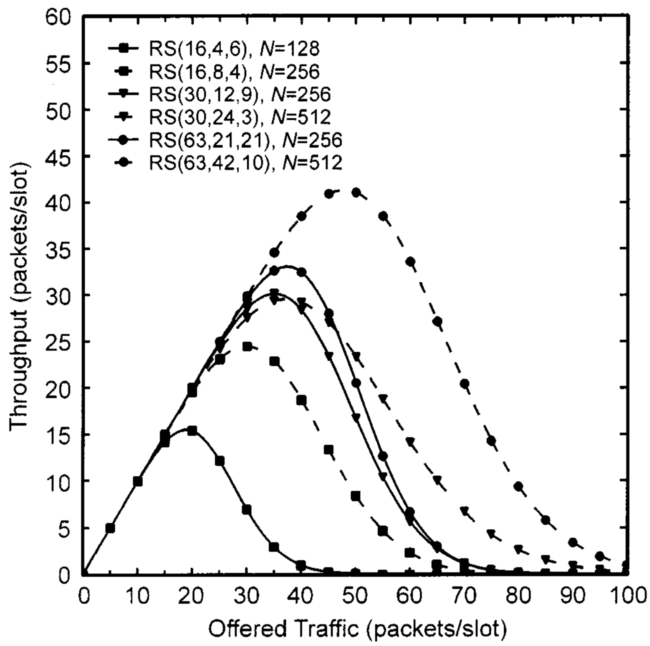

Figure 6. Throughput of single-cell data-oriented systems under Rician fading for various RS coded schemes.

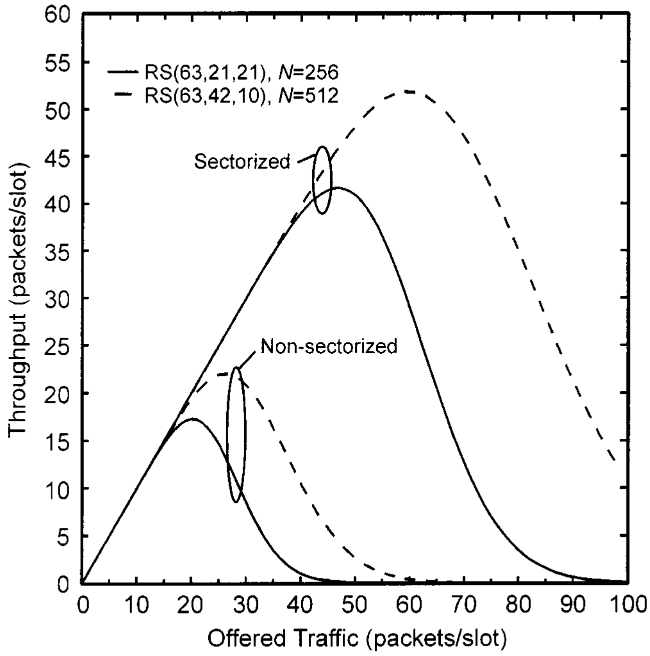

Figure 7. Throughput of multicell data-oriented systems under Rician fading for the RS(63,21,21) and RS(63,42,10) schemes.

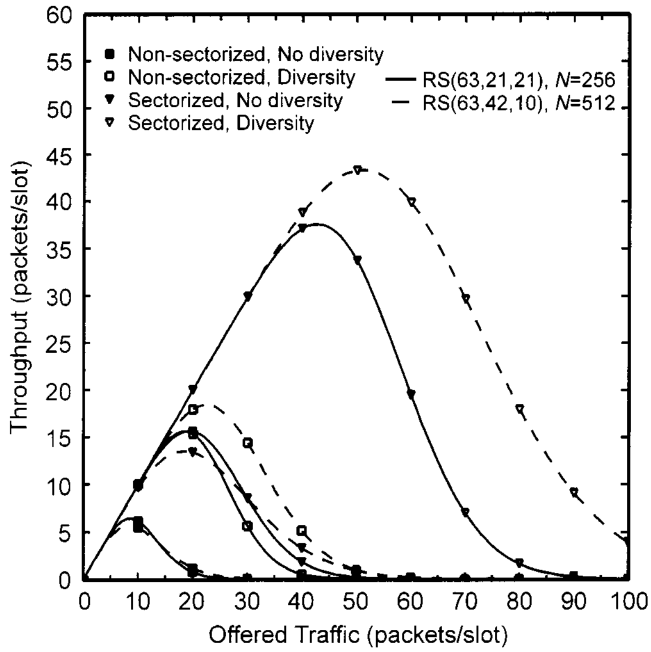

Figure 8. Throughput of multicell data-oriented systems under Rayleigh fading for the RS(63,21,21) and RS(63,42,10) schemes.

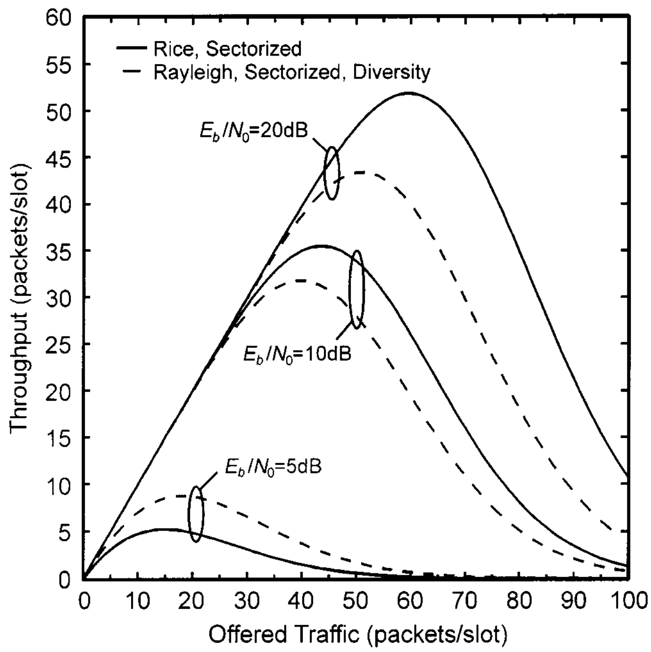

Figure 9. Throughput of multicell data-oriented systems for the RS(63,42,10) scheme and various signal to noise ratios.

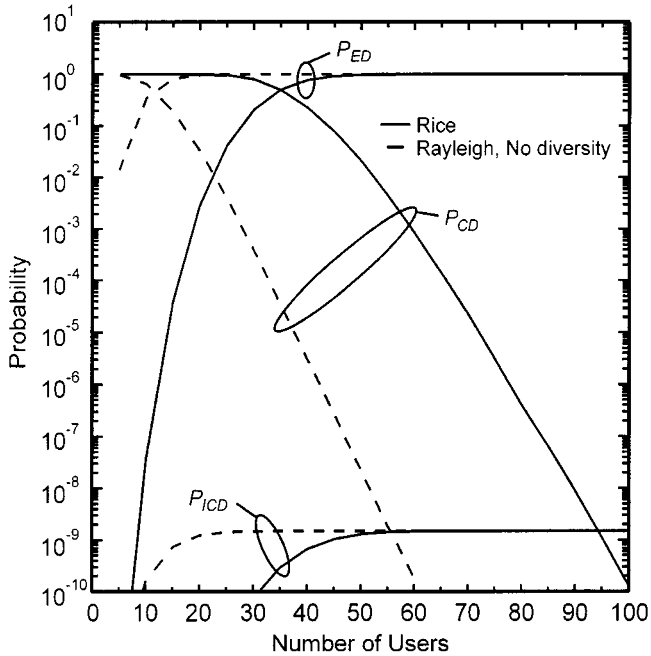

Figure 10. Correct decoding, error detection, and incorrect decoding probabilities of the RS(63,42,10) scheme under Rayleigh and Rician fading.

and incorrect decoding almost never takes place. Thus, the behavior of the RS codes is most suitable for data packet communications.

4.3. Simulation Results

In order to compare the proposed RS coded schemes with previous work, the bit error probability versus the signal to noise ratio is presented in Figure 11 for AWGN and Rayleigh environments with and without maximum output selection diversity. Similar figures were given in [7] for convolutionally encoded M-ary orthogonal signalling DS/CDMA systems. Simulation results are also presented (circled points) and highly verify the analytical results for the $RS(63, 21, 21)$ and $RS(63, 42, 10)$ codes. This latter scheme outperforms the convolutionally encoded scheme presented in [7] over 4 dB signal to noise ratios for the AWGN environment, although soft decision decoding was employed in [7]. The two RS-coded schemes behave worse in Rayleigh fading with diversity as soft decision decoding is much more effective in Rayleigh environments. The two $M = 64$ schemes proposed were found to lose 1–1.5 dB for error probabilities of 10^{-6} to 10^{-5}. This difference is not very significant when considering the simplicity of the proposed scheme (bounded distance decoding) and will probably vanish and turn into gain for the proposed schemes when properly designed error and erasures decoding or efficient soft decision decoding takes place.

5. Conclusions

The performance of RS-coded DS/CDMA with M-ary orthogonal signaling was analyzed for microcellular voice and data communications. The proposed system was found to be rather flexible, offering various different configurations that may match different systems' needs.

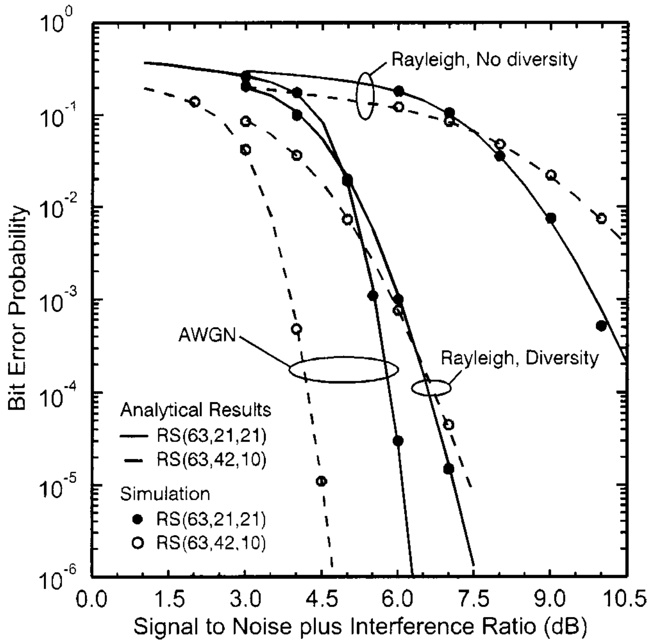

Figure 11. Analytical and simulation BEP of the RS(63,21,21) and RS(63,42,10) schemes in AWGN and Rayleigh fading environments.

Based on this fact, different services may be efficiently supported with proper coding and spreading. The increase in the symbol set size enhances performance, but the exact relationship between coding rate and spreading which gives the best results depends on the signal to noise plus interference ratio. This could be the potential for a variable coding rate and spreading strategy to increase robustness under various interference levels. Sectorization and diversity were included to improve performance, with the latter obtaining better results in certain cases.

In general, the performance achieved, either in terms of BEP or throughput, was found to be satisfactory for the fading environments considered. Almost 75 users can be accommodated effectively per cell for voice communications under Rayleigh fading. This number increases to 160 users for sectorized systems. Slightly lower values were found for Rician fading, although these values are expected to drop when imperfect interleaving and power control are encountered. When these imperfections were considered in [8], 56 users was the maximum achieved capacity derived from simulation under similar fading conditions and convolutionally encoded DS/CDMA with M-ary orthogonal signaling. With regard to data communications, maximum normalized throughput values (S/η) in the order of $0.15 - 0.17$ and $0.35 - 0.42$ were achieved for nonsectorized and sectorized systems, respectively. Because of the enhanced performance at high signal to noise ratios (or low error probabilities) that are desired, RS-coded DS/CDMA with M-ary orthogonal signaling suits data applications very well.

The proposed RS-coded DS/CDMA system with M-ary orthogonal coding was found to consist of a strong candidate for microcellular communications. The presented results (that may further improve by errors and erasures decoding) are satisfactory for either voice or data communications while preserving moderate receiver complexity. Further investigations and simulations, concerning nonperfect interleaving, other environments, diversity, decoding techniques, etc. must be considered in the future to complete the perspective of RS-coded DS/CDMA systems with orthogonal signaling in cellular communications.

Appendix

In this appendix, the probabilities of error detection and incorrect decoding of RS-coded systems are reproduced from [15] for compactness. Note that these probabilities can be exactly calculated because of the known weight distribution of RS codes.

$$\begin{aligned} P_{ICD} &= \sum_{h=d_c}^{n} P_{ICD}(h) \\ &= \sum_{h=d_c}^{n} \sum_{s=0}^{t} \sum_{i=h-s}^{h+s} \sum_{r=r_1}^{r_2} \binom{h}{h-s+r} \binom{s-r}{k-h+s-2r} \\ &\quad \times \binom{n-h}{r} (M-2)^{i-h+s-2r} (M-1)^r Q(i) A_h \end{aligned} \tag{35}$$

where $d_c = n - k + 1$ is the distance of the code, $r_1 = \max\{0, k - h\}$ and $r_2 = \left\lfloor \frac{k-h+s}{2} \right\rfloor$. $Q(i)$ is the probability of occurrence of a particular weight-i error pattern given by

$$Q(i) = \frac{P_S^i (1 - P_S)^{n-i}}{(M-1)^i} \tag{36}$$

where P_S is the symbol error probability before decoding. A_h is the weight distribution of the code, given by

$$A_h = \binom{n}{h} (M-1) \sum_{j=0}^{h-d_c} (-1)^j \binom{h-1}{j} M^{h-d_c-j}. \tag{37}$$

The probability of error detection is simply given by

$$P_{ED} = 1 - P_{CD} - P_{ICD} \tag{38}$$

References

1. K.S. Gilhousen et al., "On the Capacity of a Cellular CDMA System", *IEEE Trans. Vehic. Technol.*, Vol. 40, No. 2, pp. 303–312, 1991.
2. M.G. Jansen and R. Prasad, "Capacity, Throughput, and Delay Analysis of a Cellular DS CDMA System With Imperfect Power Control and Imperfect Sectorization", *IEEE Trans. Vehic. Technol.*, Vol. 44, No. 1, pp. 67–75, 1995.
3. P.K. Enge and D.V. Sarwate, "Spread-Spectrum Multiple Access Performance of Orthogonal Codes: Linear Receivers", *IEEE Trans. Commun.*, Vol. COM-35, No. 12, pp. 1309–1319, 1987.
4. K. Pahlavan and M. Chase, "Spread-Spectrum Multiple Access Performance of Orthogonal Codes for Indoor Radio Communications", *IEEE Trans. Commun.*, Vol. 38, No. 5, pp. 574–577, 1990.
5. M. Chase and K. Pahlavan, "Performance of DS-CDMA Over Measured Indoor Radio Channels Using Random Orthogonal Codes", *IEEE Trans. Vehic. Technol.*, Vol. 42, No. 4, pp. 617–624, 1993.
6. A.J. Viterbi et al., "Performance of Power-Controlled Wideband Terrestrial Digital Communication", *IEEE Trans. Commun.*, Vol. 41, No. 4, pp. 559–569, 1993.
7. L.F. Chang et al. "Comparison of Two Convolutional Orthogonal Coding Techniques for CDMA Radio Communications Systems", *IEEE Trans. Commun.*, Vol. 43, No. 6, pp. 2028–2037, 1995.

8. A. Jalali and P. Mermelstein, “Effects of Diversity, Power Control, and Bandwidth on the Capacity of Microcellular CDMA Systems”, *IEEE Journal on Selec. Areas in Commun.*, Vol. 12, No. 5, pp. 952–961, 1994.
9. L.M.A. Jalloul and J.M. Holtzman, “Performance Analysis of DS/CDMA with Noncoherent M-ary Orthogonal Modulation in Multipath Fading Channels”, *IEEE Journal on Selec. Areas in Commun.*, Vol. 12, No. 5, pp. 862–870, 1994.
10. E.K. Hong et al., “Performance Evaluation of DS-CDMA System with M-ary Orthogonal Signaling”, *IEEE Trans. Vehic. Technol.*, Vol. 45, No. 1, pp. 57–63, 1996.
11. A.C. Iossifides and F-N. Pavlidou, “Performance Evaluation of DS/CDMA Systems Using M-ary Orthogonal Coding Over Indoor Fading Channels”, in *Proc. PIMRC’97*, Helsinki, Finland, pp. 693–697, 1997.
12. M-H. Fong et al., “Concatenated Orthogonal/PN Spreading Sequences and Their Application to Cellular DS-CDMA Systems with Integrated Traffic”, *IEEE Journal on Selec. Areas in Commun.*, Vol. 14, No. 3, pp. 547–558, 1996.
13. R. Prasad, *CDMA for Wireless Personal Communications*, Artech House, Inc., 1996.
14. B.D. Woerner and W.E. Stark, “Trellis-Coded Direct Sequence Spread-Spectrum Communications”, *IEEE Trans. Commun.*, Vol. 42, No. 12, pp. 3161–3170, 1994.
15. J.G. Proakis, *Digital Communications*, 2nd edn., McGraw-Hill, 1989.
16. A.M. Michelson and A.H. Levesque, *Error-Control Techniques for Digital Communication*, John Wiley & Sons, 1985.
17. E. Geraniotis and J.W. Gluck, “Coded FH/SS Communications in the Presence of Combined Partial-Band Interference, Noise Jamming, Rician Nonselective Fading, and Multiuser Interference”, *IEEE Journal on Selec. Areas in Commun.*, Vol. SAC-5, pp. 194–214, 1987.
18. A.M.Y. Bigloo et al., “A Robust Rate-Adartive Hybrid ARQ Scheme for Frequency-Hopped Spread-Spectrum Multiple-Access Communication Systems”, *IEEE Journal on Selec. Areas in Commun.*, Vol. 12, No. 5, pp. 917–924, 1994.
19. R.J.C. Bultitude and G.K. Bedal, “Propagation Characteristics on Microcellular Urban Mobile Radio Channels at 910 MHz”, *IEEE Journal on Selec. Areas in Commun.*, Vol. 7, No. 1, pp. 31–39, 1989.
20. D.L. Noneaker and M.B. Pursley, “On the Chip Rate of CDMA Systems with Doubly Selective Fading and Rake Reception”, *IEEE Journal on Selec. Areas in Commun.*, Vol. 12, No. 5, pp. 853–861, 1994.
21. G-T. Chyi et al., “On the Symbol Error Probability of Maximum-Selection Diversity Reception Schemes Over a Rayleigh Fading Channel”, *IEEE Trans. Commun.*, Vol. 37, No. 1, pp. 79–83, 1989.

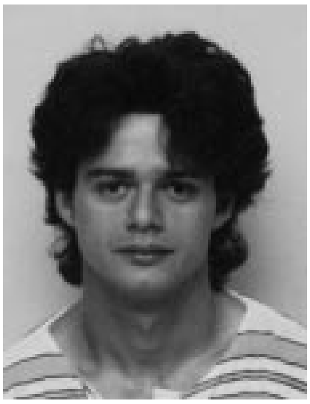

Athanassios C. Iossifides was born in Alexandroupolis, Greece, in 1969. He received his diploma in Electrical Engineering in 1994 from Aristotle University of Thessaloniki, Greece. He is currently working toward his Ph.D. degree at Aristotle University of Thessaloniki. He is involved in European COST programs concerning mobile satellite or terrestrial communications and he has served as a temporary professor for the Technological Institute of Thessaloniki for two years. His main research interests lie in the area of terrestrial and satellite mobile communications with emphasis on CDMA applications and channel coding techniques.

Fotini-Niovi Pavlidou received the diploma and the Ph.D. degree in Electrical Engineering in 1979 and 1988 respectively from the Aristotle University of Thessaloniki, Greece. She is now with the Department of Electrical and Computer Engineering at the same institution where she offers courses on Mobile Communications and Telecommunications Networks. She is involved in EU and national research projects on mobile satellite communications, ATM switching and transmission and telematics applications. Her research interests include mobile communications and high speed networking applications.